FOREX Publication
Open Access | Rapid and quality publishing
International Journal of Electrical and Electronics Research (IJEER)
Research Article | Volume 12, Issue 3 | Pages 1029-1035 | e-ISSN: 2347-470X

# Experimental analysis of an Interleaved Boost Converter for Electric Vehicle Applications

**B. Ganesh Babu[1*] and M. Surya Kalavathi[2]**

[1]*Department of Electrical and Electronics Engineering, VNR Vignana Jyothi Institute of Engineering and Technology, Hyderabad-500090, India;2ghanib@gmail.com*
[2]*Department of Electrical and Electronics Engineering, Jawaharlal Nehru Technological University, Hyderabad- 500085, India;*

*Correspondence: B. Ganesh Babu; *2ghanib@gmail.com*

**ABSTRACT-** With its potential to improve fuel efficiency and contribute to a more sustainable energy future, electric cars will be an integral part of the transportation system of the future. For the time being, this industry is using traditional boost converters. A proposal for an interleaved boost converter for EVs is made in this article. When contrasted with the Classic boost converter, the suggested one produces higher-quality results. In this proposed work, we use a two-phase boost converter to lower the output waveform's ripple current, which is often rather significant in boost converters. It is suggested to use an Interleaved Boost Converter with MPPT to maintain a steady DC output voltage from PV systems. Electric vehicle propulsion performance and system current ripple are both enhanced by the suggested integrated circuit. A comparison was made between the traditional boost converter and the proposed converter. The simulation is conducted in MATLAB/SIMULINK, considering different irradiance and temperature values. A prototype for a 1kW PV system with a resistive load is then created. To ensure the precision and efficiency of the suggested approaches, we provide simulation and experimental findings.

**Keywords:** Boost converter, Interleaved boost converter, Electrical vehicles, MPPT.

**ARTICLE INFORMATION**
**Author(s)**: B. Ganesh Babu and M. Surya Kalavathi;
**Received**: 21/07/2024; **Accepted**: 03/09/2024; **Published**: 10/09/2024;
**e-ISSN**: 2347-470X;
**Paper Id**: IJEER 2107-21;
**Citation:** 10.37391/ijeer.120337
**Webpage-link**:
https://ijeer.forexjournal.co.in/archive/volume-12/ijeer-120337.html





## 1. INTRODUCTION

These days, air pollution is a problem for all living things. The rising cost of petroleum products and the number of automobiles on the road are the primary sources of air pollution, which affects around 14% of India's population. In highly populated metropolitan areas, air pollution and greenhouse gas emissions are major concerns. The transportation industry is a major contributor to carbon dioxide emissions and is responsible for about 1.3 million fatalities annually as a result of the global use of fossil fuels [1]. Green transportation options that do not rely on fossil fuels are in high demand as a result of rising fuel prices, environmental consciousness, and the rapid depletion of natural resources [2]. Some have looked at electric cars as a greener alternative to ICEs, or vehicles powered by internal combustion engines, and a potential solution to the world's pollution and radiation problems [3]. The typical electric vehicle propulsion system consists of a high voltage DC-link connecting the electric energy alimentation circuit to the traction system [4]. In recent years, fuel-cell electric cars have emerged as a formidable alternative to conventional automobiles, and their prominence is only growing [5]. Due to its hard electrolyte, low temperature, compact size, and weight, proton exchange membrane fuel cells are one of the current fuel cell technologies that have attracted attention in constructing fuel cell electric cars [6,7]. Fuel cell engines boost DC-DC converters, energy storage elements, and bidirectional DC-DC converters make up the power supply system of fuel cell electric vehicles (FCEVs) [8,9]. However, to power critical voltage systems, like the power train system of an electric car, the electrical system must use a low-voltage fuel cell. To get the voltage up to a few hundred volts, a DC-DC boost converter is required for an economical and suitable vehicle drive system [10]. The little DC bus voltage of this power source cannot meet the minimum voltage requirement of the three-phase inverter, which generates 380 V to drive the electric motor, without a DC-DC boost converter. Therefore, the DC-DC converter stands out due to its high efficiency and voltage gain over a wide range of output powers [11-12]. The input current ripple has poor performance due to its low efficiency and short lifespan, as previously shown in studies [13]. As a result, several articles have previously discussed various approaches to addressing previous issues, increasing voltage gain, and decreasing input current ripple [14]. Thanks to these advantages, the interleaved DC-DC boost converter is being considered as a potential link between fuel cells (units, tanks) and DC buses in the automobile industry. Less input-current ripple, less current strain on the semiconductor appliances, increased density, and supernal efficacy are all benefits of this interleaved approach that are also present in the formal boost converter [15]. Many traditional boost converters make up an interleaved DC-DC boost converter; these are called phases or legs, and they are connected in parallel and share a DC connection. To reduce power loss and inactive element capacity and size, the universal input current is divided into separate phases [16]. A second leg,

FOREX Publication
Open Access | Rapid and quality publishing
International Journal of
Electrical and Electronics Research (IJEER)
Research Article | Volume 12, Issue 3 | Pages 1029-1035 | e-ISSN: 2347-470X

or compensating leg, is included in the Buck-based converter in reference [17] to reduce voltage output ripple to a minimum. A state-space averaging (SSA) analysis was used to examine the dynamic behaviour, which provided the transfer function that was used to construct the control method. According to Reference [18], a fuel cell (FC) or reformer power source may provide a multi-phase interleaved boost converter that is used in very dynamic transportation applications. The Hamiltonian function method is considered in a control theory. All of the aforementioned converter topologies are distinct from the one suggested in this study. An approach to design and development of an interleaved DC/DC boost converter for use with fuel cells in automotive applications using the dSPACE DS1104 platform, which is controlled by an FPGA board, and is linked to real-time cards. Building power converters using interleaved parallel linked converters has several benefits, such as minimizing ripple amplitude and increasing ripple frequency in the output and input waveforms, and canceling out ripples to the greatest possible degree in both the input and output waveforms. Connecting converters in parallel also improves dependability and fault tolerance, decreases the need for maintenance, and so on. To tackle all these problems at once would be too much for a traditional boost DC-DC converter. Despite its widespread use in fuel cell (FC) applications, the high current ripples coming out of the cell have many drawbacks, including increased fuel consumption, accelerated catalyst loss and carbon-support corrosion, shorter lifetime, and annoying tripping in overload situations. This is all because it can operate in the current control mode in a continuous conduction mode (CCM), which improves FC efficiency. However, one potential solution to these problems is the interleaved boost DC-DC converter, or IBC. Interleaving methods indeed enhance dependability, modularity, and power capability. High efficiency, ripple reductions, tiny filter components, and flexibility for degraded operating mode are some of the reasons why the IBC is seen as a desirable option.

The major contributions of this research work are as follows

- This paper presents the simulation and hardware implementation of an interleaved boost converter (IBC) for electric vehicle (EV) battery charging applications.
- It incorporates P&O MPPT for extracting maximum power from the PV system at different irradiance conditions.
- The proposed methodology is mathematically modeled and simulated using MATLAB/Simulink 2023a version.
- Compared to conventional boost converter, the IBC incorporates an additional control topology that facilitates current injection through interleaved stage sharing, thereby mitigating current imbalances during charging cycles.
- Furthermore, a prototype hardware model has been developed to empirically assess the performance of the proposed converter.

This research paper is organized as follows: *Section 2* describes the proposed system and its modes of operation. *Section 3* discusses the results of the simulations and the hardware prototype model. Finally, *section 4* provides the conclusions of the research.

## 2. TEST SYSTEM

The proposed system with a block diagram is shown in *figure 1*. The EV system is fed from the solar PV system, IBC, and Multi-level inverter (MLI). The battery storage system is connected at the midpoint of IBC and MLI [3]. By using IBC, the overall performance of the system gets improved. The IBCs are connected between the solar PV panel and Cascaded Multilevel Inverter (CMI), the purpose is to maintain constant DC voltage for the inverter irrespective of the solar radiation [1]. EVs are having integration of these converters with motors. The literature does not deal with optimization techniques to eliminate predominated harmonics in the integrated circuit.

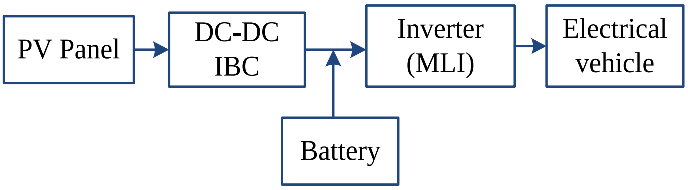


**Figure 1.** Block diagram of the proposed arrangement

### 2.1. Solar panel

In the PV-connected EVs, the IBC is connected to a solar PV array that may connect to the top of the vehicles or a solar power generation station. The PV system consists of ten series modules with twenty parallel strings with an open circuit voltage of 36.3 V and a short circuit current of 7.84 A and produces a power of 215 W [13]. The solar cell equivalent circuit is depicted in *figure 2*. It employs the P&O MPPT technique for extracting the maximum power [10]. The current equation for the PV cell can be obtained by equation (1). The IV and PV curve of the proposed PV system is shown in Fig. 3. The PV array's power output peaks at approximately 48,000 W at 25°C and around 40,000 W at 45°C, as shown in the P-V characteristics plot. This indicates that higher temperatures reduce the array's efficiency and power output. The I-V characteristics also demonstrate that current output decreases more gradually at higher temperatures. These observations highlight the importance of temperature management in optimizing PV system performance. The solar cell acts as the voltage source. It generates current when light hits it. The diode allows current to flow in one direction only. This protects the circuit from damage caused by reverse current flow. The resistor limits the current flow in the circuit.

$$I = I_p - I_d - I_s \tag{1}$$

Here, $I_p$ = Photo current, $I_d$ = diode current, $I_s$ = shunt current.

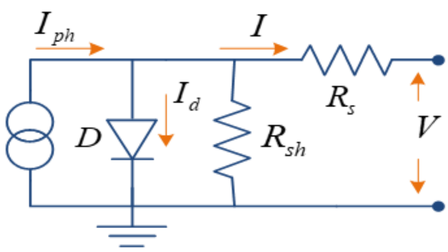


**Figure 2**. Equivalent circuit of solar cell

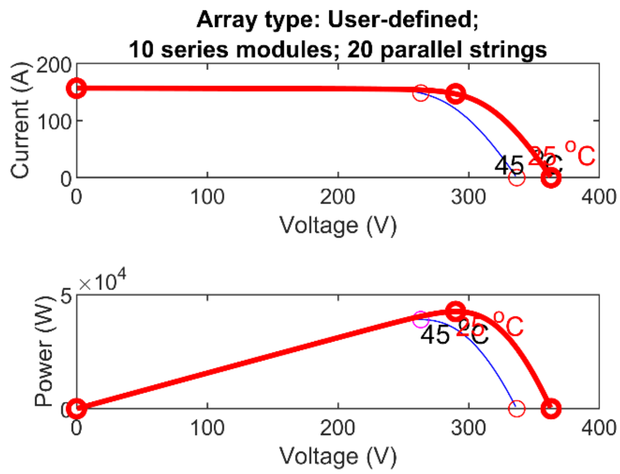


**Figure 3.** IV and PV curves of the proposed solar PV system

## 2.2 Interleaved boost converter

A boost converter (BC) can produce the higher variable average output voltage from constant input DC voltage. In BC, there are some limitations on-duty ratio to obtain greater voltage. To overcome those limits IBC has been proposed. IBC is the parallel combination of BC. In IBC, the input current ripple, output voltage ripple, and size of the component reduce and improve transient response compared to conventional BC. Interleaving also refers to the multi-phasing method used for reducing the filter size. It contains 'n' single boost converters connected parallel to each other. IBC has two control switches which are operated by a phase shift of $180^0$ and each boost converter operates in two modes, *i.e.*, Mode-1 is charging of the inductor in this mode switch is on current passes in the circuit. Mode-2 is the discharging of the inductor in this mode switch is an opened diode that makes the conduction path [11]. The below *figure 4* shows the circuit diagram of the IBC [4]. The test system parameters are presented in *table 1*.

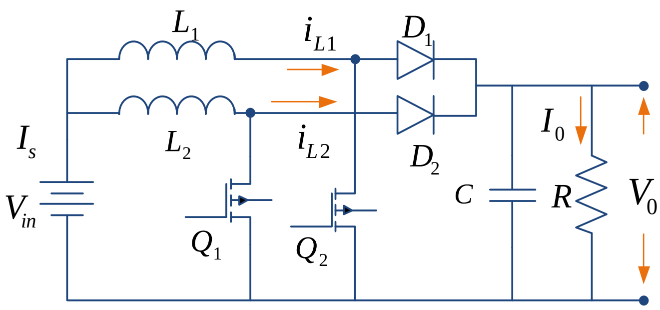


**Figure 4.** Proposed interleaved boost converter for EV application

***Mode -1:*** In mode1 switch $Q_1$ is ON, allowing current to flow from $V_{in}$ through inductors $L_1$ and $L_2$, storing energy in these inductors. Switch $Q_2$ is OFF, and diodes $D_1$ and $D_2$ are reverse-biased, so no current flows to the output. The energy is stored in $L_1$ and $L_2$ without being transferred to the capacitor *C* or load *R*.

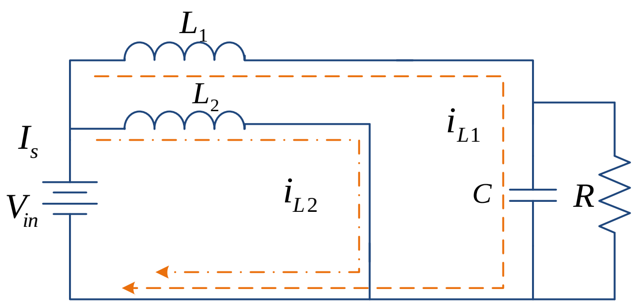


**Figure 4 (a)** Mode.1 operation when Q1 is on

***Mode -2:*** When $Q_1$ is OFF and $Q_2$ is ON, current flows from $V_{in}$ through inductors $L_1$ and $L_2$, and switches $Q_2$. Inductors $L_1$ and $L_2$ store energy during this mode. Diodes $D_1$ and $D_2$ are reverse-biased, so no current reaches the output. Thus, no energy is transferred to the capacitor *C* or load *R*. The inductor currents $IL_1$ and $IL_2$ are depicted in the *figure 4(c)*.

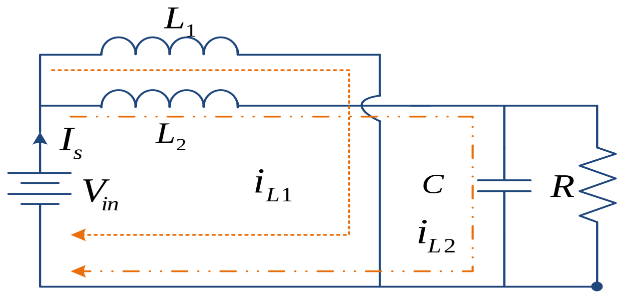


**Figure 4 (b)** Mode.2 operation when $Q_1$ is off and $Q_2$ on.

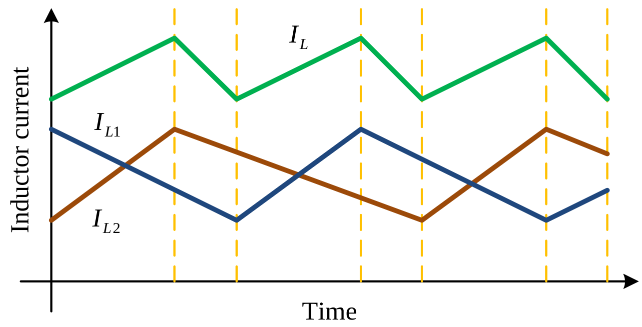


**Figure 4 (c)**. Ideal waveform for the interleaved converter

The following parameters are helpful to study the performance of IBC under steady-state analysis. The design of different elements is considered from the reference [18], and duty cycle, input and output current ripple equations are shown below.

**Duty cycle:** it can determine the output voltage at different values of *D*. The range of *D* lies between 0 to 1.

$$v0 = \frac{v_{dc}}{1-D} \quad (2)$$

Here $V_o$=output voltage, *V* = input voltage, *D* = duty ratio.

***Input Current:*** The input current supply is given by *equation (3)*

$$I_{in} = \frac{P_{in}}{V} \quad (3)$$

***Inductor Current Ripple:*** The difference between two inductor currents is called inductor current ripple [1] `

$$\Delta I_1 I_2 = \frac{V.D}{f.L} \quad (4)$$

Here the *L*= inductance of inductors and *f*= input switching frequency.

**Table 1. Test system parameters simulation**

| Parameter | Value |
|---|---|
| Input voltage | 77.97 V |
| Switching frequency | 25 kHz |
| Inductor | 2.5 mH |
| Capacitor | 78 µF |
| Resistor | 10 |

# 3. RESULTS AND ANALYSIS

This section describes the simulation and experimental results of the interleaved boost converter. The results include input current, input voltage, output voltage, inductor current, output voltage ripple, and output power, which are obtained from simulations in MATLAB and a hardware prototype.

## 3.1 Simulation results

The *figure 5*. shows the input voltage and current of IBC the input voltage is around 78V and the input current is around 30A. The input voltage shows damped oscillations and a settling time of 0.025 seconds, while the input current remains stable and constant. The PWM signals for $Q_1$ and $Q_2$ are shown in *fig. 6*. Which moves with a speed of 25 kHz.

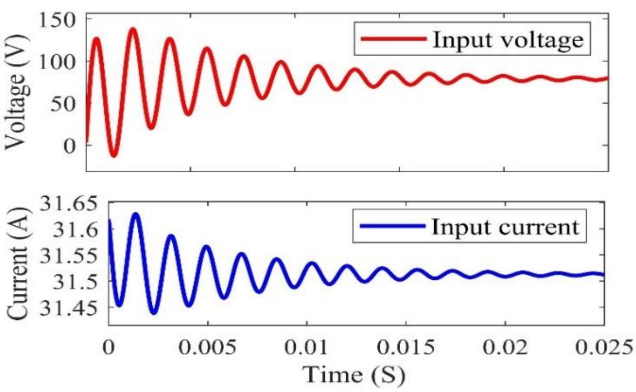


**Figure 5.** Input current and input voltage of the IBC

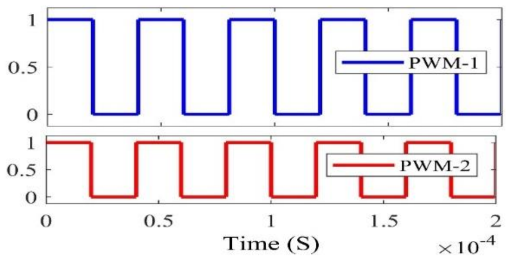


**Figure 6.** PWM Signals for Interleaved Boost Converter

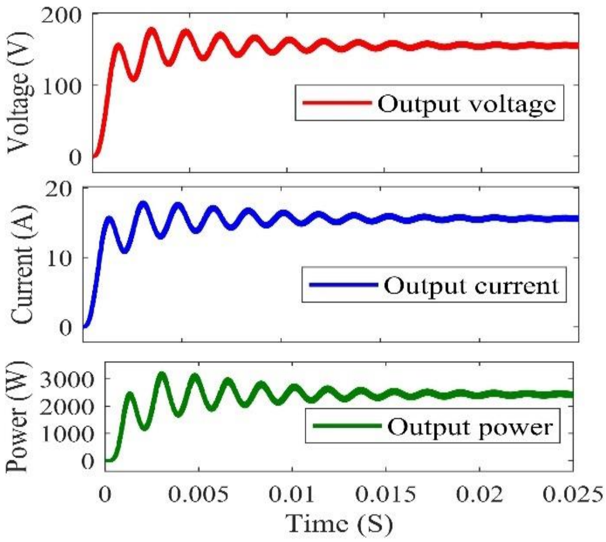


**Figure 7.** Output parameters of IBC

*Figure 7* shows the output voltage of IBC at 50% duty cycle and the value of output voltage is 158.03V, output current is 15A and output power is 2.5 kW.

## 3.2 Experimental results

The experimental setup shown in *figure 8*, operates with an input voltage of 100V. The experimental design parameters are shown in *table 2*. The switching frequency of the converter ranges from 5 to 20 kHz, controlled by an Insulated Gate Bipolar Transistor (IGBT) rated at 600V and 75A, capable of switching at up to 20 kHz. The circuit shown in *figure 4*, includes an inductor with a value of 5mH, capable of handling up to 15A of current. A diode rated at 600V and 30A is incorporated to ensure it can manage the required voltage and current levels. The converter is designed to achieve an output voltage range of up to 500V, delivering an output power of 1kW. This setup allows for efficient voltage conversion while ensuring stability and reliability during the experiment. The experimental input voltage 100V and input voltage ripple are shown in *figure 9* and *figure 10*. The input PWM signals are shown in *figure 11*, generated by using the FPGA-Spartan-6 controller. The voltage stress across the switch is shown in *figure 12*, and the output voltage and its ripple are presented in *figure 13* and *figure 14* respectively. The multi level output voltage waveform and current are depicted in *figure 15* and *figure 16* respectively.

**Table 2. Experimental parameters**

| Parameter | Specifications |
|---|---|
| Input voltage | 100V |
| Switching frequency | 5 to 20 kHz |
| Inductor | 5mH/15A |
| Diode | 600V/30A |
| IGBT | 600V,75A,20KHz |
| Output voltage Range | 500V |
| Output Power : | IKW |

FOREX Publication
Open Access | Rapid and quality publishing

International Journal of
Electrical and Electronics Research (IJEER)
Research Article | Volume 12, Issue 3 | Pages 1029-1035 | e-ISSN: 2347-470X

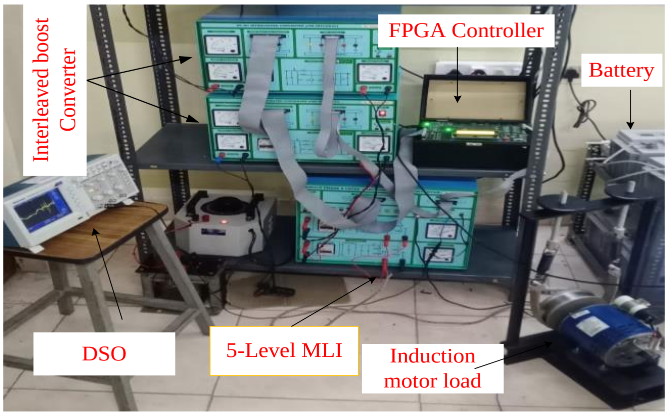


**Figure 8.** Experimental test setup of figure 1

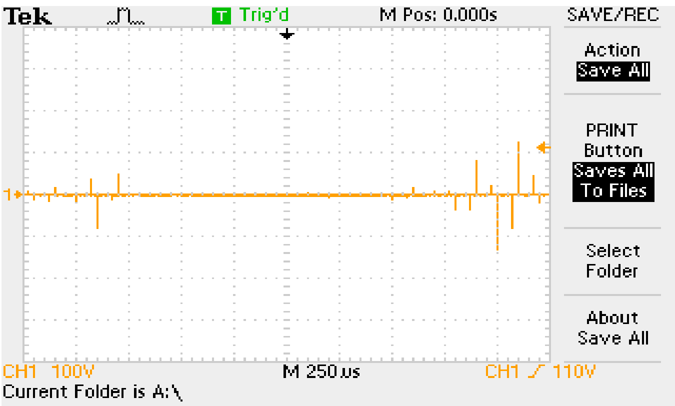


**Figure 9.** Input voltage of IBC

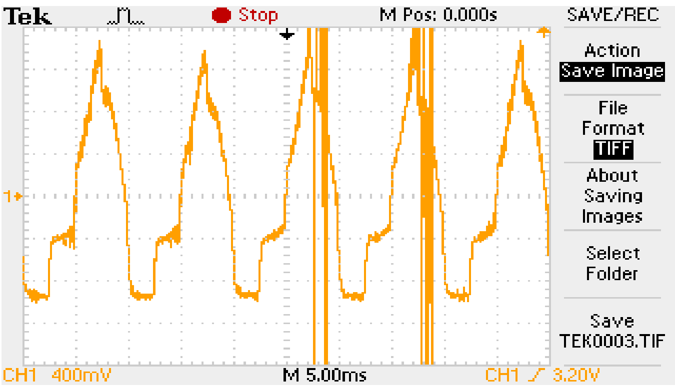


**Figure 10.** Input voltage ripple

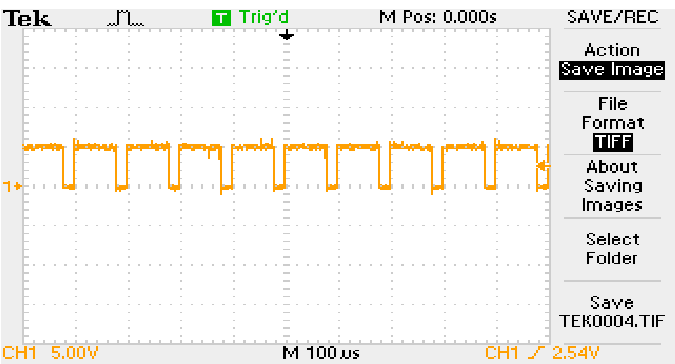


**Figure 11.** PWM Signals for IGBTs

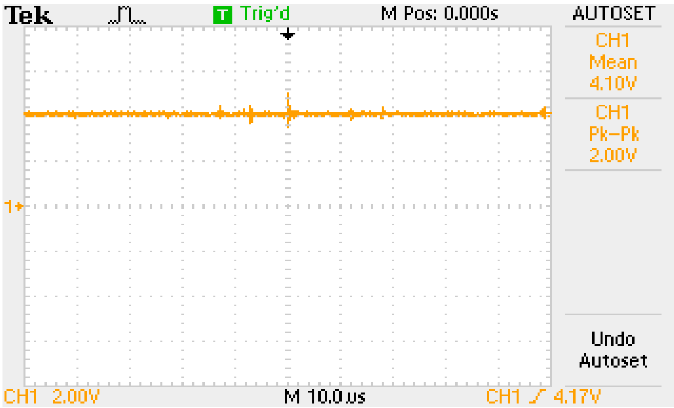


**Figure 12.** Voltage drop across the switch

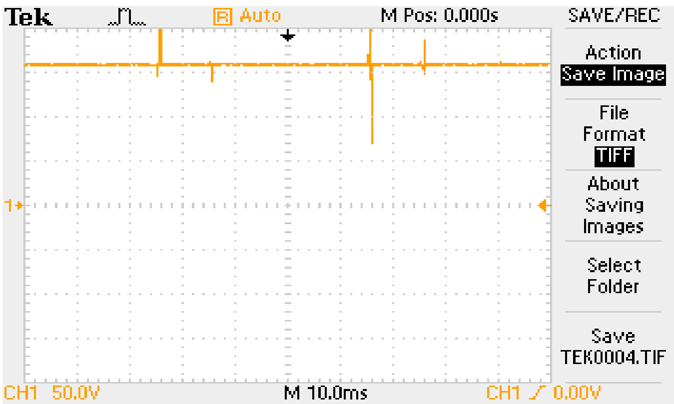


**Figure 13.** Output voltage of IBC

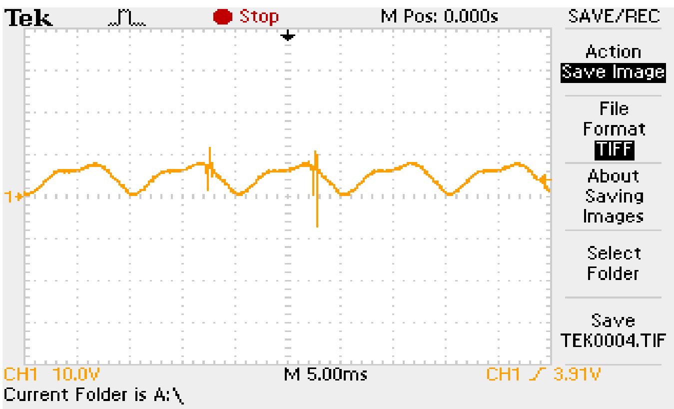


**Figure 14.** Output voltage ripple

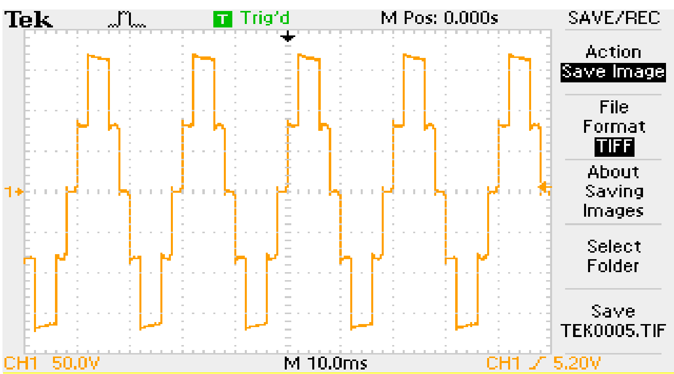


**Figure 15.** 5-level MLI output waveform

FOREX Publication
Open Access | Rapid and quality publishing

International Journal of
Electrical and Electronics Research (IJEER)
Research Article | Volume 12, Issue 3 | Pages 1029-1035 | e-ISSN: 2347-470X

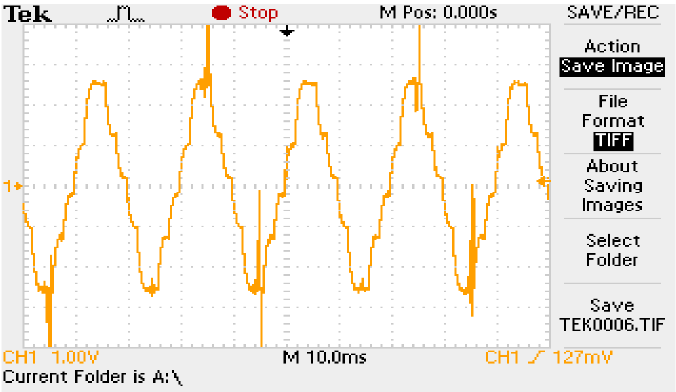


**Figure 16**. 5-level MLI current waveform

The comparison with existing methods is shown in the below *table 3*. From this table, it is found that the voltage ripple, current ripple and efficiency are much better than the conventional boost converter.

**Table 3. Comparison of results with existing boost converter**

| Converter | Boost Converter [15] | Interleaved Boost Converter |
|---|---|---|
| Output Voltage ($V_o$) | 133 V | 158 V |
| Output Voltage ripple (%) | 0.40 | 0.255 |
| Output Current ($I_o$) | 3.5075 | 3.25 |
| Output Current ripple (%) | 0.428 | 0.277 |
| Efficiency (%) | 0.953 | 0.975 |

## 4. CONCLUSION

The PWM-fed two-phase IBC technology will unquestionably improve efficiency and reliability, in addition to reducing ripple current and size in comparison to other topologies. This is because the technology is designed to be used in high-power applications to use solar photovoltaic cells. Through the simulation analysis, the goals of the current project have been accomplished, and the waveforms that were produced have been noticed. Additionally, the replies that were generated by the IBC have been evaluated. By using IBC, it is possible to conclude that the ripples in the output voltage may be decreased. The hardware findings demonstrate that the suggested technique is more successful than simulations in terms of its effectiveness. By using two switches on the circuit, the switching losses may be significantly decreased. This is because the circuit can alternate the turning on of these two switches for a greater degree of efficiency.

## REFERENCES

[1] Khalid, Muhammad. "Smart grids and renewable energy systems: Perspectives and grid integration challenges." Energy Strategy Reviews 51 (2024): 101299.

[2] X. S. Li, et al., "Analysis and Simplification of Three-Dimensional Space Vector PWM for Three-Phase Four-Leg Inverters," IEEE Transactions on Industrial Electronics, vol. 58, pp. 450-464, Feb 2011.

[3] R. Arulmozhiyal and K. Baskaran, "Implementation of a Fuzzy PI Controller for Speed Control of Induction Motors Using FPGA," Journal of Power Electronics, vol. 10, pp. 65-71, 2010.

[4] D. Zhang, et al., "Common Mode Circulating Current Control of Interleaved Three-Phase Two-Level Voltage-Source Converters with Discontinuous Space-Vector Modulation," 2009 IEEE Energy Conversion Congress and Exposition, Vols 1-6, pp. 3906-3912, 2009.

[5] Z. Yinhai, et al., "A Novel SVPWM Modulation Scheme," in Applied Power Electronics Conference and Exposition, 2009. APEC 2009. Twenty-Fourth Annual IEEE, 2009, pp. 128-131.

[6] Wen, Jun, Taotao Jin, and Keyue Smedley. "A new interleaved isolated boost converter for high power applications." In Twenty-First Annual IEEE Applied Power Electronics Conference and Exposition, 2006. APEC'06., pp. 6-pp. IEEE, 2006.

[7] Yao, Gang, Alian Chen, and Xiangning He. "Soft switching circuit for interleaved boost converters." IEEE Transactions on Power Electronics 22, no. 1 (2007): 80-86.

[8] Gules, Roger, L. Lopes Pfitscher, and L. Claudio Franco. "An interleaved boost DC-DC converter with large conversion ratio." In 2003 IEEE International Symposium on Industrial Electronics (Cat. No. 03TH8692), vol. 1, pp. 411-416. IEEE, 2003.

[9] Seyezhai, Rand, and B. L. Mathur. "Design and implementation of interleaved boost converter for fuel cell systems." International journal of hydrogen energy 37, no. 4 (2012): 3897-3903.

[10] Newlin, D. Jeba Sundari, R. Ramalakshmi, and S. Rajasekaran. "A performance comparison of interleaved boost converter and conventional boost converter for renewable energy application." In 2013 International Conference on Green High Performance Computing (ICGHPC), pp. 1-6. IEEE, 2013.

[11] Verma, Nitin, Shilpa Mishra, and Sandeep Shukla. "Implementation of solar based PWM fed two phase interleaved boost converter." In 2015 Communication, Control and Intelligent Systems (CCIS), pp. 470-476. IEEE, 2015.

[12] Pinheiro, Jose R., Hilton A. Grundling, Dalton LR Vidor, and José E. Baggio. "Control strategy of an interleaved boost power factor correction converter." In 30th Annual IEEE Power Electronics Specialists Conference. Record.(Cat. No. 99CH36321), vol. 1, pp. 137-142. IEEE, 1999.

[13] Ho, Carl Ngai-Man, Hannes Breuninger, Sami Pettersson, Gerardo Escobar, and Francisco Canales. "A comparative performance study of an interleaved boost converter using commercial Si and SiC diodes for PV applications." IEEE Transactions on Power Electronics 28, no. 1 (2012): 289-299.

[14] Thiyagarajan, A., SG Praveen Kumar, and A. Nandini. "Analysis and comparison of conventional and interleaved DC/DC boost converter." In Second international conference on current trends in engineering and technology-ICCTET 2014, pp. 198-205. IEEE, 2014.

[15] Tseng, Kuo-Ching, Chun-An Cheng, and Chun-Tse Chen. "High step-up interleaved boost converter for distributed generation using renewable and alternative power sources." IEEE journal of emerging and selected topics in power electronics 5, no. 2 (2016): 713-722.

[16] Jang, Yungtaek, and Milan M. Jovanovic. "Interleaved boost converter with intrinsic voltage-doubler characteristic for universal-line PFC front end." IEEE transactions on power electronics 22, no. 4 (2007): 1394-1401.

[17] Spiazzi, Giorgio, and Simone Buso. "Analysis of the interleaved isolated boost converter with coupled inductors." IEEE Transactions on Industrial Electronics 62, no. 7 (2014): 4481-4491.

[18] Ramesh, Adireddy, M. Siva Kumar, and O. Chandra Sekhar. "Interleaved boost converter fed with PV for induction motor/agricultural applications." International Journal of Power Electronics and Drive Systems 7, no. 3 (2016): 835.